Chlorine-mediated electrodeposition of hierarchical and hydrophobic copper electrocatalysts for efficient CO$_2$ electroreduction to ethylene

Yinqiong Wu,[a,b,‡] Jiye Feng,[a,‡] Danni Shi,[a] Wenbiao Zhang,[a,c] Yi Tang,[c] and Qingsheng Gao[a,*]

a. College of Chemistry and Materials Science, and Guangdong Provincial Key Laboratory of Functional Supramolecular Coordination Materials and Applications, Jinan University, Guangzhou 510632, P. R. China. Email: tqsgao@jnu.edu.cn

b. Shantou Power Supply Bureau of Guangdong Power Grid Co. Ltd., Shantou 515000, P. R. China

c. Department of Chemistry, Shanghai Key Laboratory of Molecular Catalysis and Innovative Materials, and Laboratory of Advanced Materials and Collaborative Innovation Centre of Chemistry for Energy Materials, Fudan University, Shanghai 200433, China.

‡ These authors contribute equally to this work.

Experimental

Materials synthesis

Cu dendrite catalysts were directly electrodeposited on a GDL electrode which was pre-treated by plasma under an O_2 atmosphere to form a micro-hydrophilic surface. In the typical synthesis of ED-Cu(Cl), the plating solution was 100 mL deionized water containing 100 mM $CuSO_4$ and 100 mM KCl. A glassy carbon electrode clip was used to fix the GDL as the cathode, a Ag/AgCl electrode as the reference electrode, and a Pt as the counter electrode. ED-Cu(Cl) was deposited under a constant potential of −0.7 V (vs. Ag/AgCl) for 2000 s, and then the product was collected and rinsed with deionized water and ethanol, and then dried in a vacuum oven at 40 °C for 1 h. For comparison, ED-Cu and ED-Cu(Br) supported on GDLs were prepared with a plating solution (100 mL) of 100 mmol L^{-1} $CuSO_4$ and that containing 100 mmol L^{-1} KBr, respectively.

Physical measurements

TEM, HR-TEM, EDS and the corresponding elemental mapping were taken on a JEOL 2100F instrument. SEM was collected on a ZEISS ULTRA55. XRD analysis was performed on Bruker D8 diffractometer with Cu Ka radiation (λ = 1.54056 Å). XPS was processed on Thermo Scientific (Escalab 250Xi), using C 1s (284.8 eV) as a reference. Water contact angles and CO_2 bubble adhesion experiments were analyzed on Kruss DSA-100 and LAUDA Scientific LSA-100, respectively. The [Ca^{2+}] of the transparent $Ca(OH)_2$ solution after collecting gaseous CO_2 were detected by using an inductively coupled plasma-optical emission spectrometer (ICP-OES, OPTIMA 2000DV).

Electrochemical measurements

All of the current densities were collected by a standard three-electrode configuration on an electrochemical workstation (CHI 760, Shanghai Chenhua), using a Ag/AgCl electrode as the reference electrode, and a platinum as the counter electrode. The applied potentials were converted to the RHE using the equation: E (vs. RHE) = E (vs. Ag/AgCl) + 0.197 V + 0.0591 × pH. For CO_2RR performance, catalysts were loaded onto GDL and tested in a flow cell (Gaoss Union). CO_2 with the flow rate of 20 mL

min^{-1} was passed through the gas chamber at the back side of the GDL (1×1 cm^2). The quantification of gaseous products was conducted on a gas chromatograph (GC). Gas-phase products were sampled every 30 min using high-purity nitrogen (N$_2$, 99.999%) as the carrier gas. The column effluent (separated gas mixtures) was first passed through a thermal conductivity detector (TCD) where hydrogen was quantified; then CO$_2$RR products was quantified by FID. According to the peak areas in GC, the FEs were calculated using the following equation:

$$FE = \frac{nxFV}{j_{total}} \times 100\%$$

where n is the number of electrons transferred, x is the mole fraction of the product, F is faradaic constant (F = 96485 C mol^{-1}), V is the total molar flow rate of gas and j$_{total}$ is the total current.
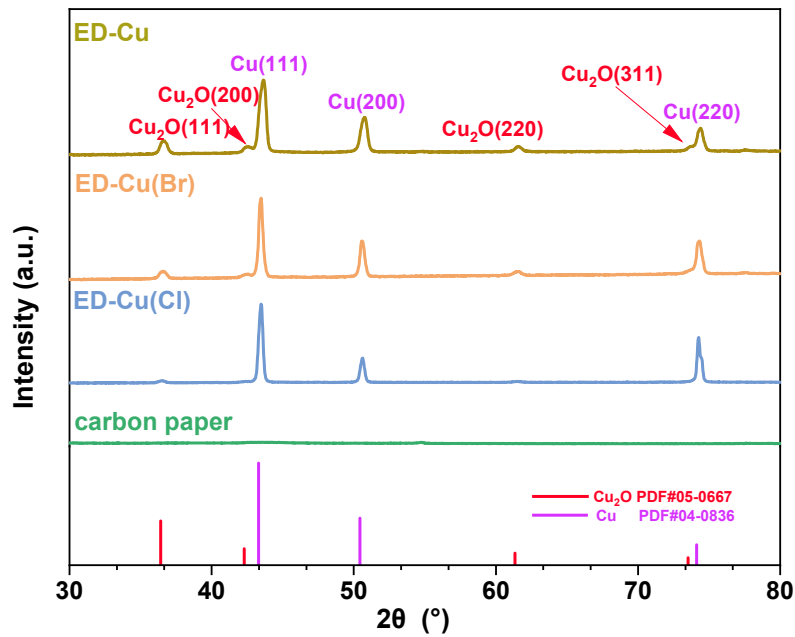
Fig. S1 (a) XRD patterns of ED-Cu, ED-Cu(Br) and ED-Cu(Cl).
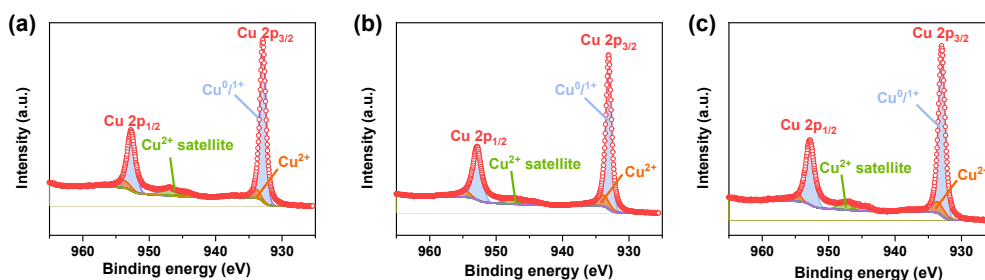
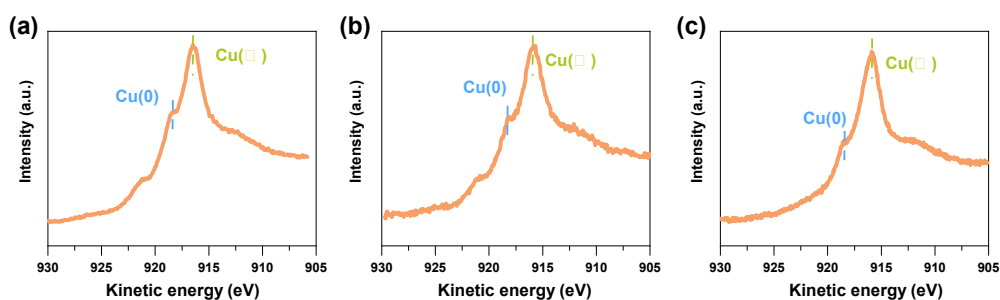**Fig. S2** Cu 2p XPS spectra of (a) ED-Cu, (b) ED-Cu(Br) and (c) ED-Cu(Cl).

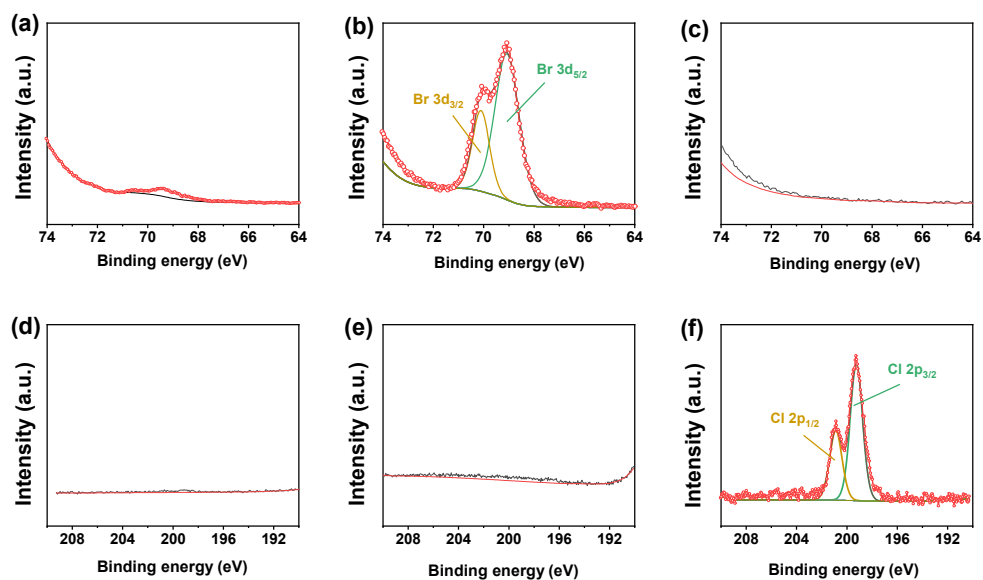**Fig. S3** Cu Auger LMM spectra of (a) ED-Cu, (b) ED-Cu(Br) and (c) ED-Cu(Cl).

Fig. S4 (a, b and c) Br 3d and (d, e and f) Cl 2p XPS spectra of (a, d) ED-Cu, (b, c) ED-Cu(Br) and (c, f) ED-Cu(Cl).
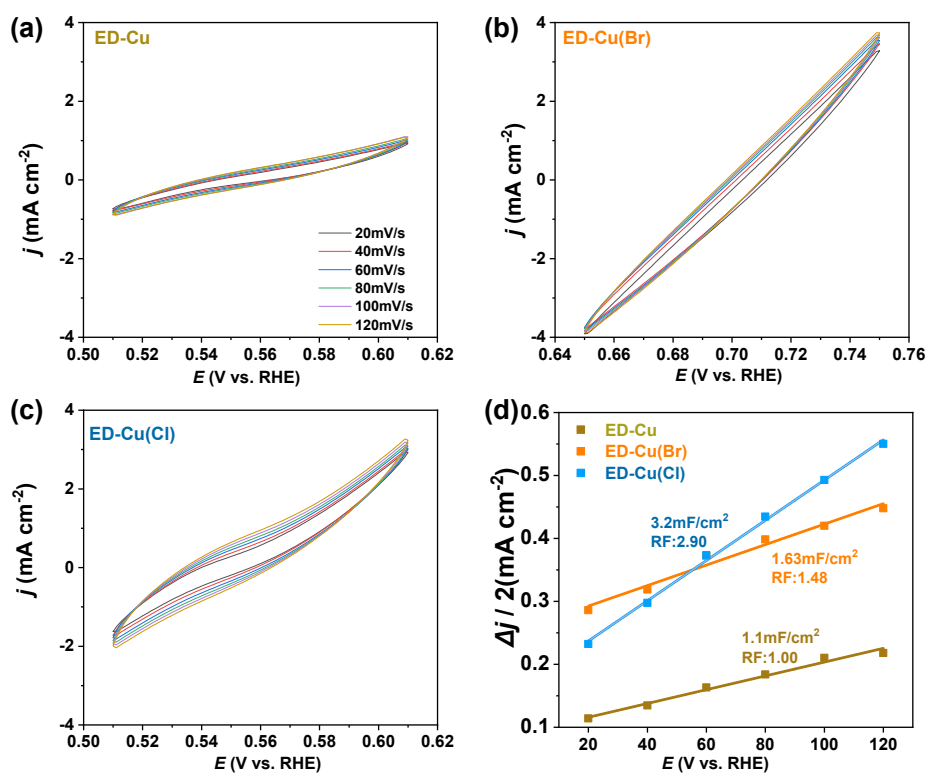
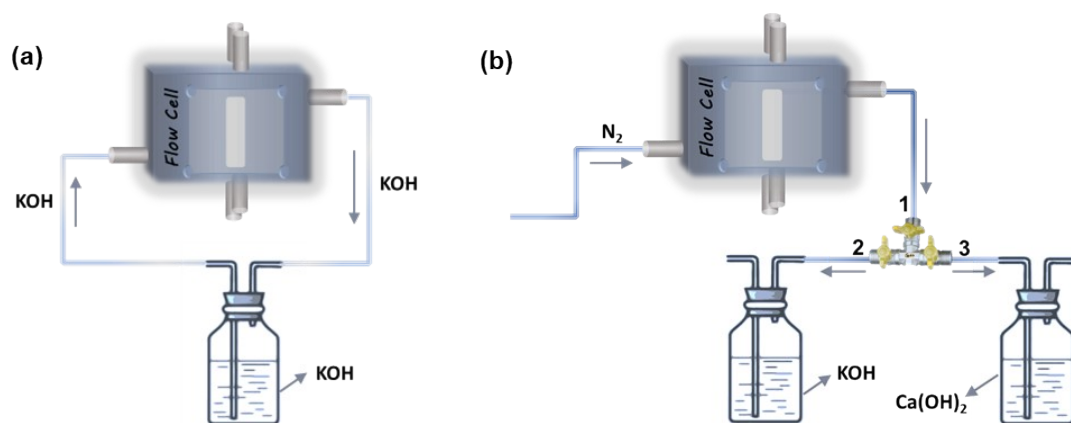**Fig. S5** (a-c) Double-layer capacitances and (d) roughness factors of ED-Cu, ED-Cu(Br) and ED-Cu(Cl) electrodes. CVs were taken over a range of scan rates in 1.0 M KOH.

Fig. S6 Illustration for the devices used for (a) CO_2RR and (b) CO_2 collection after electrochemical tests.
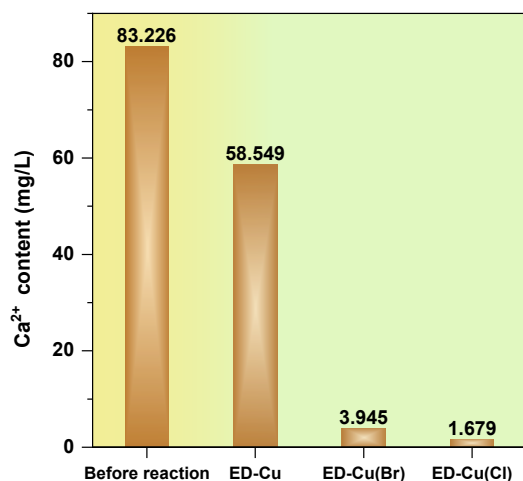
Fig. S7 $[Ca^{2+}]$ of the transparent $Ca(OH)_2$ solution after collecting gaseous CO_2 from spent ED-Cu, ED-Cu(Br) and ED-Cu(Cl). The $[Ca^{2+}]$ was determined by ICP-OES measurement.
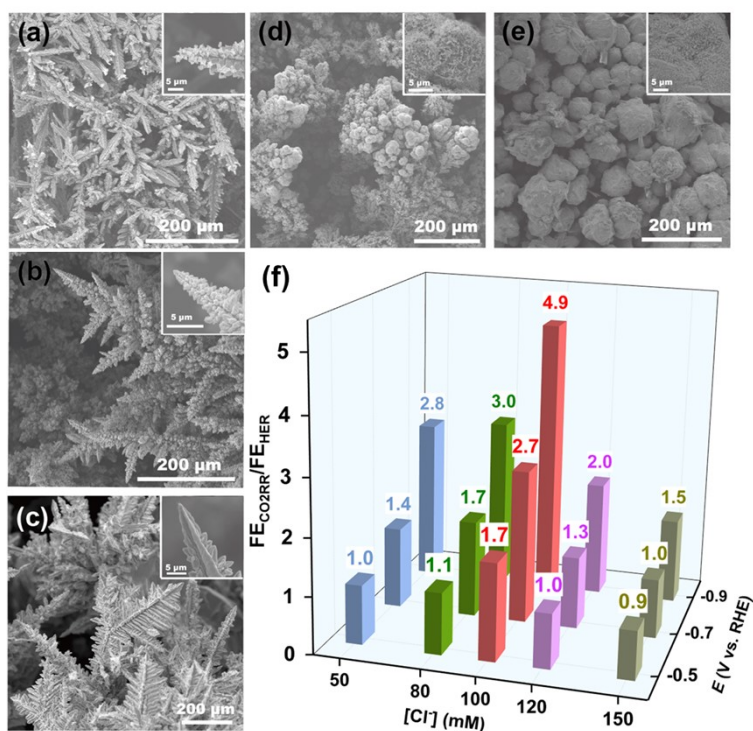

Fig. S8 SEM images of ED-Cu(Cl) received at various $[Cl^-]$ of (a) 50 mM, (b) 80 mM, (c) 100 mM, (d) 120 mM and (e) 150 mM, and (f) their FE_{CO2RR}/FE_{HER} ratios during 45 min CO_2RR test in a flow cell with 1.0 M KOH electrolyte.
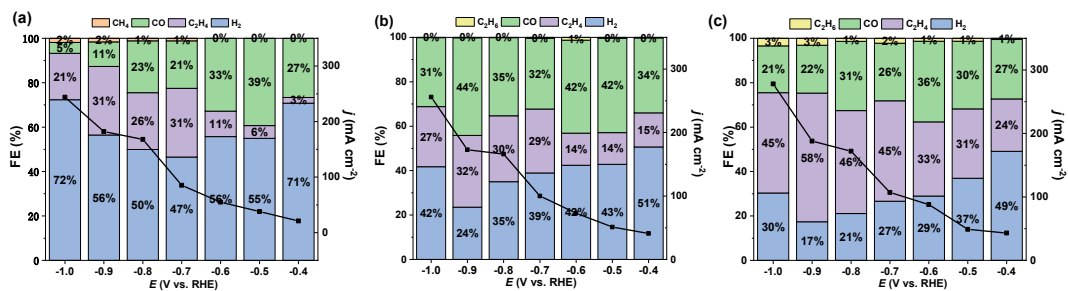
Fig S9 (a-c) CO_2RR products and H_2 distributions of (a) ED-Cu, (b) ED-Cu(Br) and (c) ED-Cu(Cl).
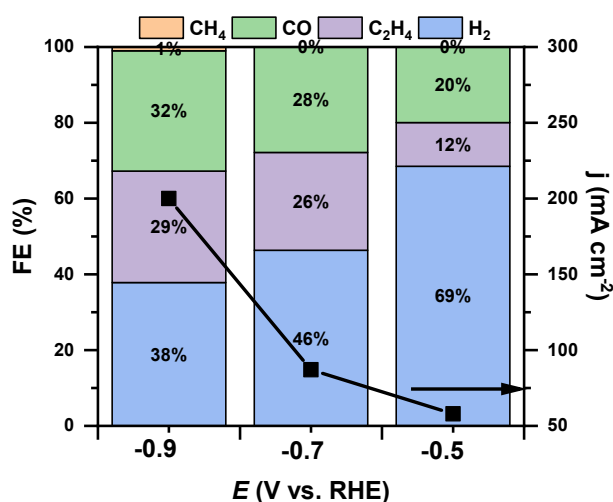

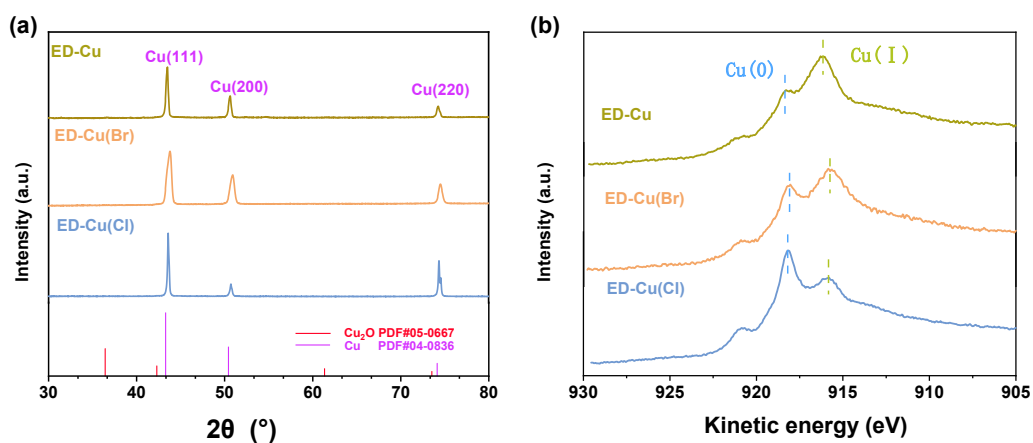**Fig. S10** CO_2RR products FEs of ED-Cu electrode immersed in the 100 mM KCl solution.

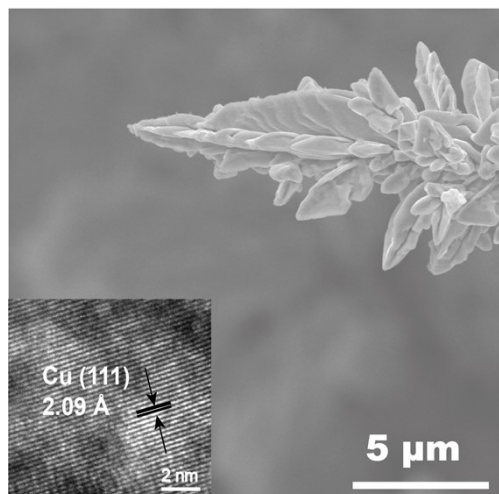**Fig. S11** (a) XRD patterns and (b) Cu Auger LMM spectra of spent ED-Cu, ED-Cu(Br) and ED-Cu(Cl) after electrolysis.

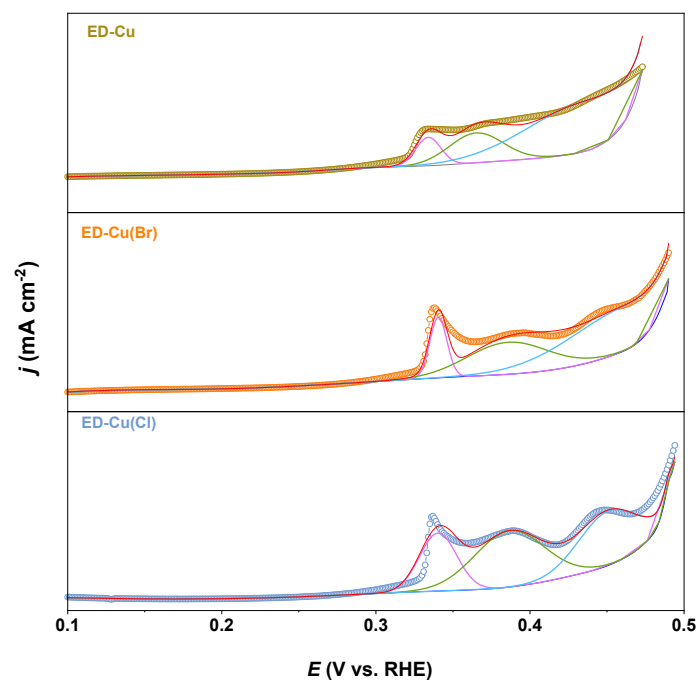**Fig. S12** SEM and (inset) HR-TEM images of spent ED-Cu(Cl) after electrolysis.

Fig. S13 The fitting of OH$^-$ desorption peaks of CVs of ED-Cu, ED-Cu(Br) and ED-Cu(Cl).
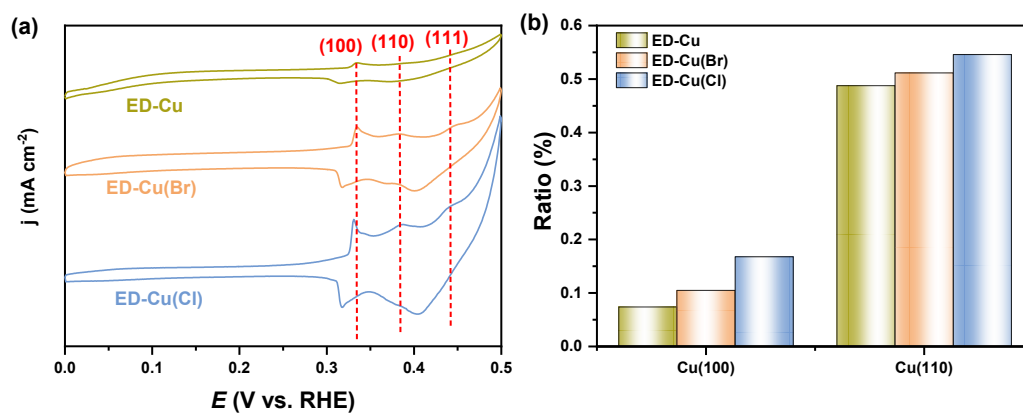
Fig. S14 (a) CV curves of ED-Cu, ED-Cu(Br) and ED-Cu(Cl) collected in 1.0 M KOH and (b) the ratio of Cu(100) and (110) relative to the sum of three basic facets (100), (110) and (111) after CO_2RR tests.